

# Research Journal of Pharmaceutical, Biological and Chemical Sciences

## Synthesis and Characterization of $\text{Cu}_x\text{Zn}_{1-x}\text{O}$ Nanocomposites

Ashwani Sharma\*, Pallavi, and Sanjay Kumar

Dept. of Physics, M.D.University, Rohtak-124001 Haryana, India

### ABSTRACT

$\text{Cu}_x\text{Zn}_{1-x}\text{O}$  ( $x = 0.1, 0.3, 0.5, 0.7, 0.9$ ) nanocomposites have been synthesized by a Sol-Gel method based on polymeric network of polyvinyl alcohol (PVA). In this method mixture solvent of 50:50 ethanol water was used to dissolve copper nitrate, zinc nitrate and PVA. The mixture was heated to  $80^\circ\text{C}$  to form homogeneous gel solution. The obtained gel was slowly heated to evaporate the solvent to form a hard homogeneous gel. The hard gel was calcinated at a temperature of  $600^\circ\text{C}$  for 4 hours and 8 hours and converted into nanocomposites. The prepared nanocomposites have been characterized using X-Ray Diffraction (XRD), SEM, FTIR, UV-VIS. In the observed spectral features, the peak position, intensity and bandwidth were related to structural properties of investigated samples. The size of nanocomposites heated at  $600^\circ\text{C}$  for 4h and 8 h were calculated using Debye-Scherrer formula. In all the samples, it was observed that particle size increases, when we increase the time of calcinations from 4h to 8 h at fixed temperature of  $600^\circ\text{C}$ . The range of nanocomposites comes out from 15.8 nm to 21.0 nm. SEM images shows nanocomposite are of spherical and uniform shape. In UV-VIS spectra, there is increase in absorption in UV region sharply and linearly in visible region in most of samples. FTIR spectra of samples is used as a unique collection of absorption bands to confirm the presence of different compounds in samples.

**Keywords:-** Nanocomposites, Synthesis, XRD, FTIR, UV-VIS, SEM

*\*Corresponding author*



## INTRODUCTION

Nano form of matter exhibit different properties from bulk on account of quantum confinement effect. This behavior of nanomaterials has created interest in the development and study of properties of nanomaterials. The physical and chemical properties of nanomaterials depend on their size and shape.[1-2] Due to large surface to volume ratio of nanoparticles, their properties electrical, optical, chemical, mechanical and magnetic can be selectively controlled by the size, morphology and composition of the particles. In recent years, there has been great interest in the study of zinc oxide doped nanocomposites with other metals. ZnO nanoparticles are of great importance because of their unique electrical, optical, gas sensing properties and having large bonding energy. Due to its low cost and other properties like good electrical, optical, nontoxic behavior, it has many applications in different fields like solar cells, gas sensors, spintronics, ultraviolet lasers etc. CuO is a p-type semiconductor and has unique properties and have wide applications in many fields such as gas sensors, photo catalyst and electrochemistry.[3,4].

Among other compound semiconductors, copper oxide is of great Interest in semiconductor physics. Copper forms two well-known stable oxides, cupric oxide [CuO] and cuprous oxide [Cu<sub>2</sub>O]. These two oxides have different physical properties, different colors, crystal structures and electrical properties. There are many reasons why CuO is chosen for sensing applications .CuO has many promising applications due to its unique features like high specific surface area, chemical stability, electrochemical activity, high electron communication features [5]. . Cuprous oxide is mostly p-type, direct band gap, II-VI semiconductor with band gap of ~2 eV and cupric oxide has a monoclinic crystal structure and presents p- type semiconductor behavior with a indirect band gap of 1.21 – 1.51 eV. CuO has been used as a basic material in High-Tc superconductors as the super-conductivity in these classes of systems is associated with Cu-O bondings [6-8]. The possibility of low cost production methods and the good electrochemical properties make CuO to be one of the best materials for electrical, optical, sensing and so forth. It is also used as CO oxidation of automobile exhaust gases. [9]

## EXPERIMENTAL

In this work mixed ethanol- water solvent[50:50] was used to dissolve 2 gm zinc nitrate, 2 gm copper nitrate and 8 gm PVA, the mixture was heated to 80°C to form a homogeneous sol solution. The obtained sol was slowly heated to evaporate the solvent and it form a hard homogeneous gel. The Pyrolysis of the final gel was performed at a temperature of 600°C for 4 hours and 8 hours. During the Pyrolysis process the PVA polymeric network through the outer surface , zinc and copper nitrate salts in appropriate amount simultaneously calcinated and converted into Cu<sub>x</sub>Zn<sub>1-x</sub>O nano composites. The obtained sample was crushed to prepare fine powder.

## RESULTS AND DISCUSSION

### XRD Studies:-

The XRD pattern of  $\text{Cu}_x\text{Zn}_{1-x}\text{O}$  nanocomposites shown in fig [1-4] which were calcinated at  $600^\circ\text{C}$  for 4 hours and 8 hours were obtained using panalytical's Xpert-pro powder diffractometer employing  $\text{Cu}-\text{K}-\alpha$  radiations in the  $2\theta$  range  $10^\circ-90^\circ$ . The particle size of as prepared samples were found using Scherrer formula using Scherrer formula

$$d = 0.9\lambda / \beta \cos\theta$$

Where  $d$  = average partice size,  $\beta$  is full width at half maxima [FWHM],  $\theta$  is the Bragg angle,  $\lambda$  is the wavelength of  $\text{Cu K}$  in radians [10-12]

The particle size of the samples is given in table 1.

It is seen that the particle size increases in all the samples when we increase the time of calcinations from 4h to 8h at  $600^\circ\text{C}$  except one having  $X=0,5$ .

TABLE 1

Time of Calcination	Sample $\text{Cu}_x\text{Zn}_{1-x}\text{O}$ [X=0.1] No1	Sample $\text{Cu}_x\text{Zn}_{1-x}\text{O}$ [X=,0.3] No 2	Sample $\text{Cu}_x\text{Zn}_{1-x}\text{O}$ [X=0.5] No3	Sample $\text{Cu}_x\text{Zn}_{1-x}\text{O}$ [X=0.7] No4	Sample $\text{Cu}_x\text{Zn}_{1-x}\text{O}$ [X=0.9] No5
4 hours	15.8 nm	16.7 nm	16.8 nm	16.8 nm	16.8 nm
8 hours	21.1 nm	20.8 nm	14.0 nm	21.0 nm	21.0 nm

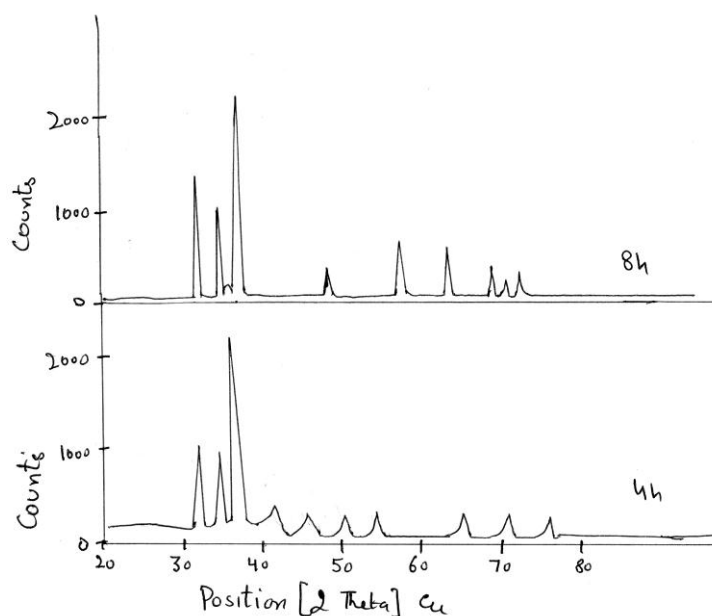


Fig 1 XRD pattern of  $\text{Cu}_x\text{Zn}_{1-x}\text{O}$  [X= 0.1] Nanocomposite

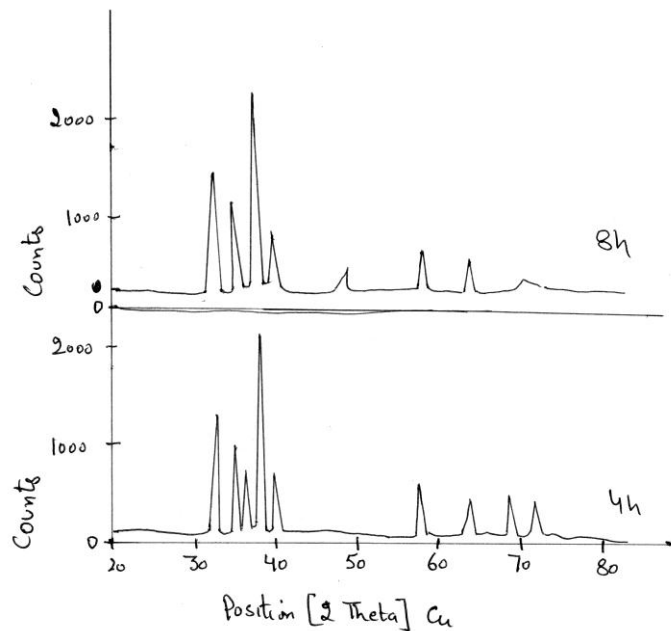


Fig 2 XRD pattern of  $Cu_xZn_{1-x}O$  [X= 0.3] Nanocomposite

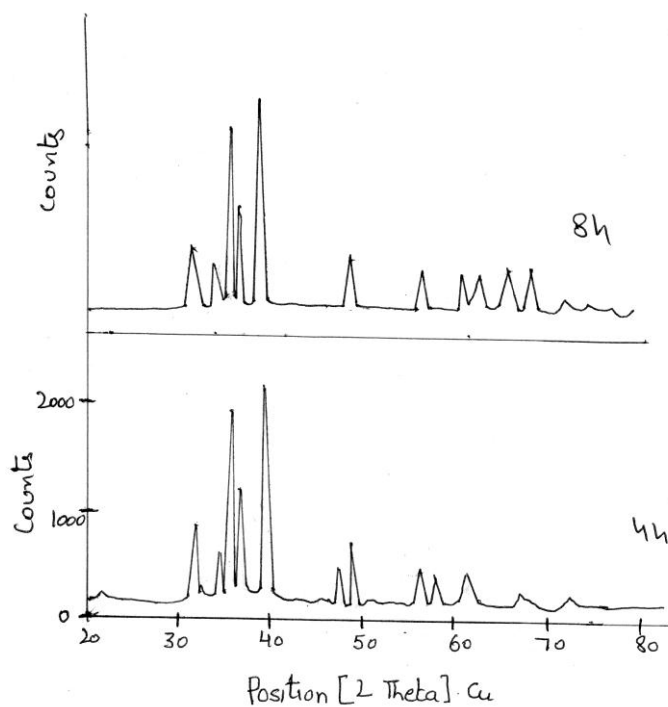


Fig 3 XRD pattern of  $Cu_xZn_{1-x}O$  [X= 0.5] Nanocomposite

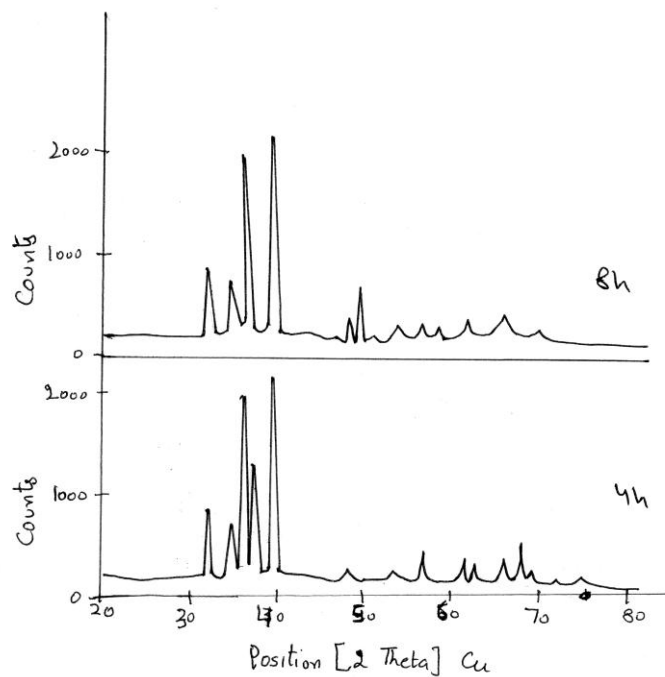


Fig 4 XRD pattern of  $Cu_xZn_{1-x}O$  [X= 0.7] Nanocomposite

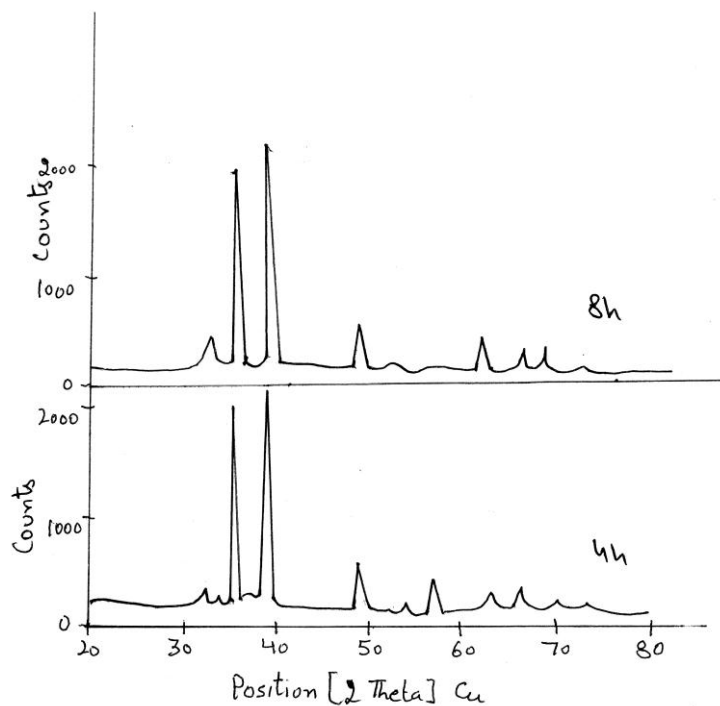


Fig 5 XRD pattern of  $Cu_xZn_{1-x}O$  [X= 0.9] Nanocomposite

SEM:-

SEM images of  $\text{Cu}_x\text{Zn}_{1-x}\text{O}$  [ $X= 0.1,0.9$ ] Nanocomposites annealed for 4h and 8 h at  $600^\circ\text{C}$  are shown in fig [6-9] SEM image demonstrate the morphology of nanoparticles which were synthesized through Sol-Gel method. The images indicate that the particle of the nanocomposite are uniform, regular, spherical They reveal the formation of Nano Crystalline material and shows randomly oriented aggregates of the size ranges from 14.0 to 21.1 nm. When more copper is added [ $X=0.9$ ], there is porous network due to rapid release of gases by-products during the combustion. The particle size increases when we increase the time of calcinations from 4h to 8 h at  $600^\circ\text{C}$  [13]

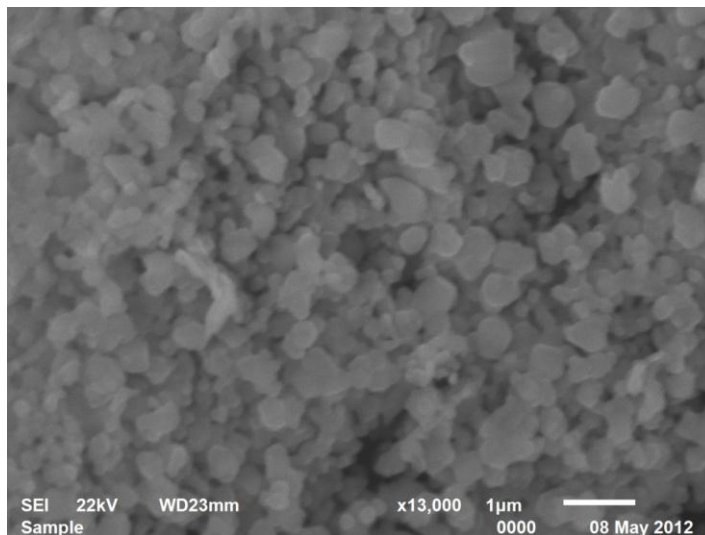


Fig 6: SEM image of  $\text{Cu}_x\text{Zn}_{1-x}\text{O}$  [ $X= 0.1$ ] annealed at  $600^\circ\text{C}$  for 4h

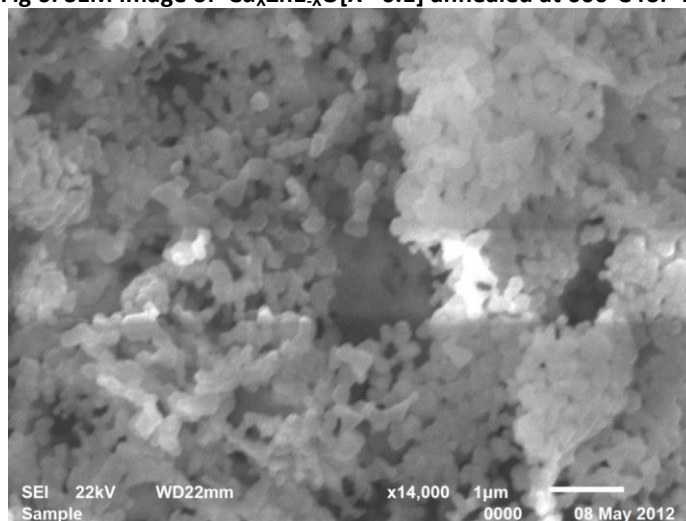
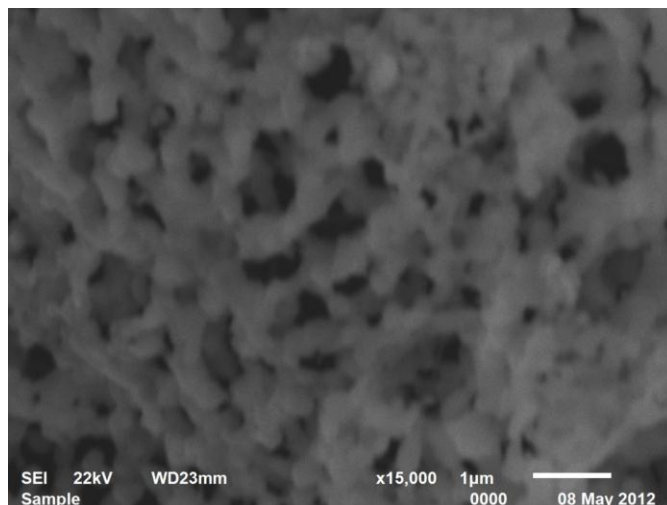
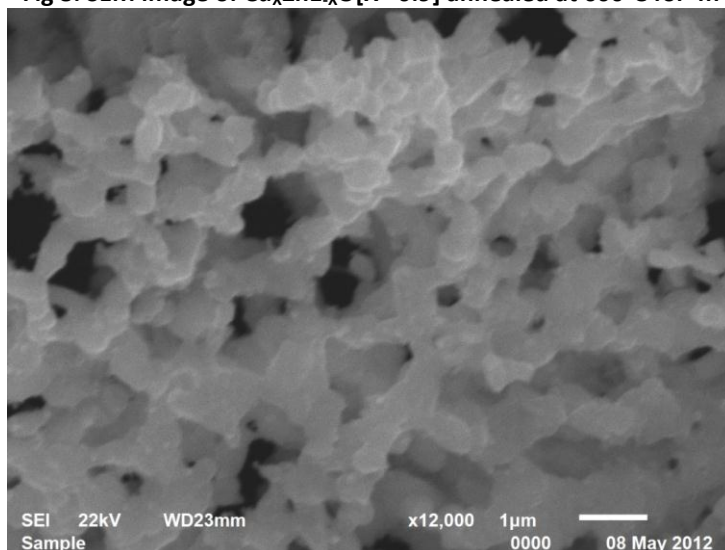


Fig 7: SEM image of  $\text{Cu}_x\text{Zn}_{1-x}\text{O}$  [ $X= 0.1$ ] annealed at  $600^\circ\text{C}$  for 8h



**Fig 8: SEM image of  $\text{Cu}_x\text{Zn}_{1-x}\text{O}$  [X= 0.9] annealed at 600°C for 4h**



**Fig 9: SEM image of  $\text{Cu}_x\text{Zn}_{1-x}\text{O}$  [X= 0.9] annealed at 600°C for 8h**

### UV-VIS Spectrul Studies:

The UV-VIS study of nanocomposites  $\text{Cu}_x\text{Zn}_{1-x}\text{O}$  [X= 0.1, 0.3,0.5,0.7,0.9] were done using Hitachi 330 spectrophotometer in the wavelength range 200 to 800 nm. The spectra of nanocomposites are shown in fig [10-14] All samples shows absorption edges which are blue shifted. The blue shift of absorption edge arises due to quantum confinement effect of nanoparticles. . Absorption of  $\text{Cu}_x\text{Zn}_{1-x}\text{O}$  [X=0.1] nanocomposites when heated at 600°C for 4 h increases sharply in UV region and then increases linearly in visible range. Absorption in  $\text{Cu}_x\text{Zn}_{1-x}\text{O}$  [X=0.1] nanocomposites when heated at 600°C for 6 h increases sharply in ultraviolet region and then decreases in visible region. In sample  $\text{Cu}_x\text{Zn}_{1-x}\text{O}$  [X=0.3] nanocomposites when heated at 4h and 6h at 600°C shows similar results. In sample  $\text{Cu}_x\text{Zn}_{1-x}\text{O}$  [X=0.5] nanocomposites when heated at 600°C for 4 h and 6 h, there is increase in absorption



linearly in both the region of ultraviolet and visible. Sample  $\text{Cu}_x\text{Zn}_{1-x}\text{O}$  [ $X=0.7$ ] when heated at  $600^\circ\text{C}$  for 4 h and 6h shows same result as of sample having  $X=0.5$ . In sample  $\text{Cu}_x\text{Zn}_{1-x}\text{O}$  [ $X=0.9$ ] there is increase in absorption with less slop in both region when heated at  $600^\circ\text{C}$  for 4 h and increases with great slop when heated at  $600^\circ\text{C}$  for 8 h[14] Thus it is observed that in all the samples, absorption increases first in ultraviolet region and then in visible region with different slopes.

UV spectra provides information about optical band gap of the material. The energy band of the material is related to the absorption coefficient  $\alpha$  by the Tauc relation  $\alpha h\nu = A[h\nu - E_g]^2$  where A is constant,  $h\nu$  is photon energy.  $E_g$  is band gap and  $n = 1/2$  for allowed direct transition. Plotting a graph between  $[\alpha h\nu]^2$  and  $h\nu$  gives the value of band gap. The extrapolation of the straight line to  $[\alpha h\nu]^2 = 0$  gives the value of band gap as shown in fig[15-16] for  $\text{Cu}_x\text{Zn}_{1-x}\text{O}$  [ $X=0.5$ ] calcinated at 4h and 8h. It is seen from the graph that the value of band gap decreases when we increase the time of calcinations from 4h to 8h.

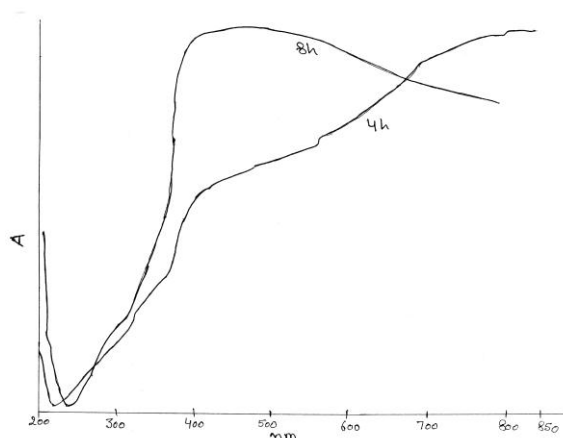


Fig 10: UV-VIS Spectra of  $\text{Cu}_x\text{Zn}_{1-x}\text{O}$ [ $X=0.1$ ] calcinated at  $600^\circ\text{C}$  for 4h and 8h 1

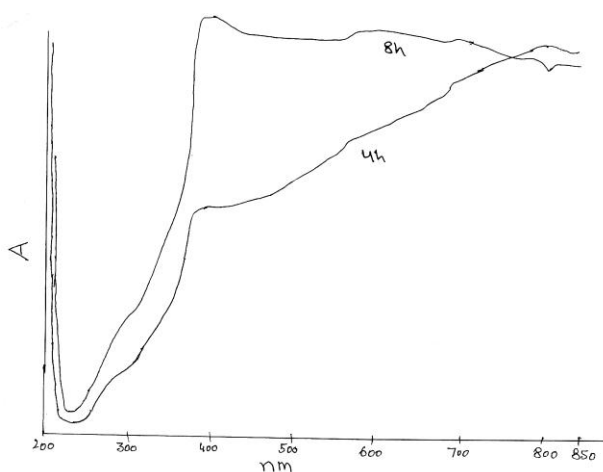


Fig 11: UV-VIS Spectra of  $\text{Cu}_x\text{Zn}_{1-x}\text{O}$ [ $X=0.3$ ] calcinated at  $600^\circ\text{C}$  for 4h and 8h2



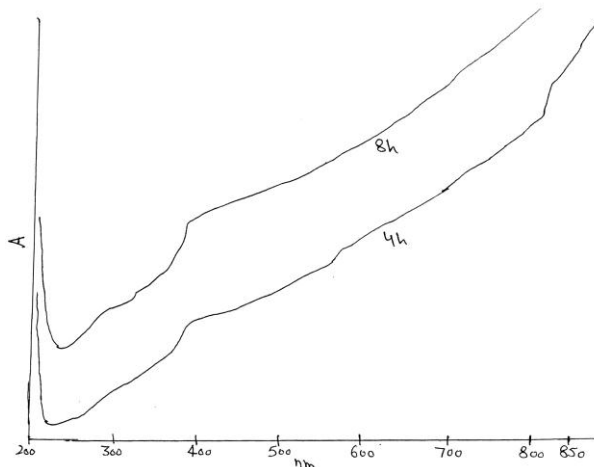


Fig 12: UV-VIS Spectra of Fig 13  $\text{Cu}_x\text{Zn}_{1-x}\text{O}$  [X= 0.7] calcinated at  $600^\circ\text{C}$  for 4h and 8h 4

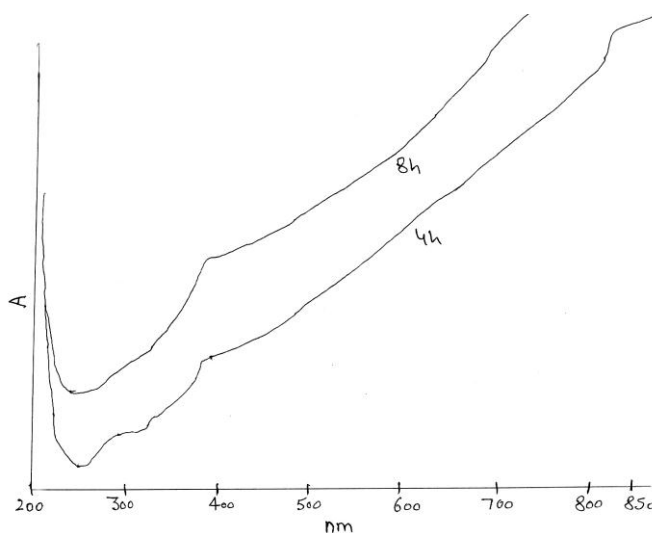


Fig 13: UV-VIS Spectra of  $\text{Cu}_x\text{Zn}_{1-x}\text{O}$  [X= 0.7] calcinated at  $600^\circ\text{C}$  for 4h and 8h 5

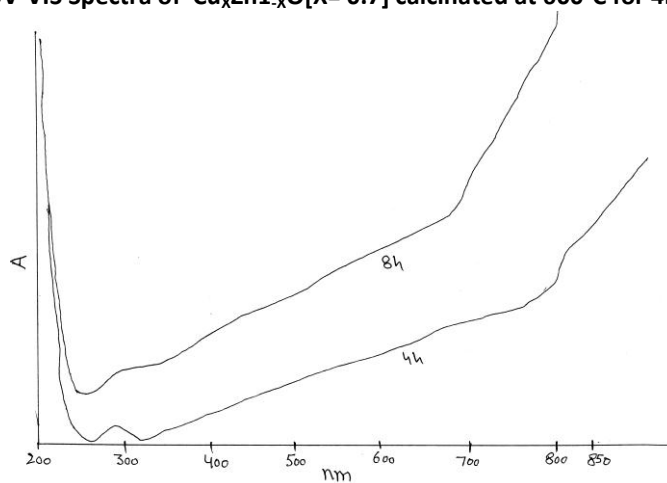


Fig 14: UV-VIS Spectra of  $\text{Cu}_x\text{Zn}_{1-x}\text{O}$  [X= 0.1] calcinated at  $600^\circ\text{C}$  for 4h and 8h 3

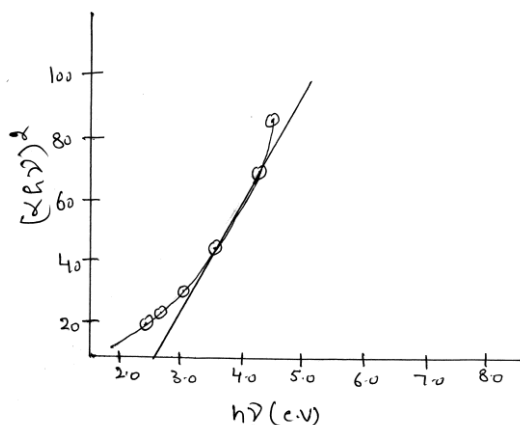


Fig 15: Graph between  $[\alpha hv]^2$  and  $h\nu$  for  $Cu_xZn_{1-x}O$  [x=0.5] for 4 h.

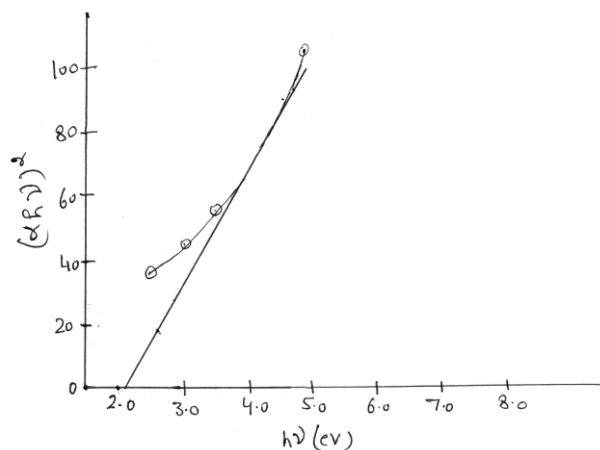


Fig 16: Graph between  $[\alpha hv]^2$  and  $h\nu$  for  $Cu_xZn_{1-x}O$  [x=0.5] for 8 h.

### FTIR Spectra Analysis:

The infrared spectroscopic[IR] study of the nanocomposites were done using Perkin Elmer –Spectrum RX FTIR Spectrophotometer in the wave number range  $400-4000\text{cm}^{-1}$ . The FTIR spectra of  $Cu_xZn_{1-x}O$  [X= 0.1, 0.3,0.5,0.7,0.9] are shown in fig [17-21]. FTIR spectra of all samples annealed at  $600^\circ\text{C}$  for 4 h and 8 h shows transmission peaks nearly at  $3400\text{cm}^{-1}$ ,  $2920\text{cm}^{-1}$ ,  $1437\text{cm}^{-1}$ ,  $1050\text{cm}^{-1}$ ,  $550\text{cm}^{-1}$  and  $480\text{cm}^{-1}$ . In  $Cu_xZn_{1-x}O$  [X= 0.1] when annealed at  $600^\circ\text{C}$  for 4 h and 8h, new peaks were observed at  $2853\text{cm}^{-1}$ ,  $1632\text{cm}^{-1}$ ,  $445\text{cm}^{-1}$ .

In  $Cu_xZn_{1-x}O$  [X= 0.3] when annealed at  $600^\circ\text{C}$  for 4 h, new peaks were observed at  $3502\text{cm}^{-1}$ ,  $1115\text{cm}^{-1}$ ,  $619\text{cm}^{-1}$  and when annealed at  $600^\circ\text{C}$  for 8 h ' new peaks were observed at  $1628\text{cm}^{-1}$ ,  $896\text{cm}^{-1}$ ,  $625\text{cm}^{-1}$  and  $531\text{cm}^{-1}$ . In  $Cu_xZn_{1-x}O$  [X= 0.5] when annealed at  $600^\circ\text{C}$  for 4 h, new peaks were observed at  $1636\text{cm}^{-1}$ ,  $1534\text{cm}^{-1}$ ,  $1275\text{cm}^{-1}$ ,  $1163\text{cm}^{-1}$ ,  $842\text{cm}^{-1}$ ,  $762\text{cm}^{-1}$  and when annealed at  $600^\circ\text{C}$  for 8 h ' new peaks were observed at  $1744\text{cm}^{-1}$ ,  $1632\text{cm}^{-1}$ ,  $1384\text{cm}^{-1}$ ,  $1276\text{cm}^{-1}$ ,  $841\text{cm}^{-1}$ . In  $Cu_xZn_{1-x}O$  [X= 0.7] when annealed at

600<sup>o</sup> C for 4 h, new peaks were observed at 1555 cm<sup>-1</sup> and when annealed at 600<sup>o</sup> C for 8 h, new peaks were observed at 1635 cm<sup>-1</sup>, 1555 cm<sup>-1</sup> and at 1164 cm<sup>-1</sup>. In Cu<sub>x</sub>Zn<sub>1-x</sub>O [X= 0.9] when annealed at 600<sup>o</sup> C for 4 h, no new peaks were observed and when annealed at 600<sup>o</sup> C for 8 h, new peaks were observed at 1548 cm<sup>-1</sup>. [15-16]

Peak near 3400 cm<sup>-1</sup> corresponds to the [O-H] mode of water molecule [17]. The peak around 2900 cm<sup>-1</sup> is due to C-H bond. Another peak near 1630 cm<sup>-1</sup> may be due to H-O-H bending vibrational mode due to absorption of water in air. The weak absorption peak at around 1600 cm<sup>-1</sup> corresponds to presence of small amount of residual carbon in the sample. Band around 1450 cm<sup>-1</sup> corresponds to asymmetric stretching of C=O bonds. Bands around 1100 cm<sup>-1</sup> is due to C-O bonding. Bands at 619 cm<sup>-1</sup> is due to intrinsic vibration of metal oxide bond. Band observed at 619 cm<sup>-1</sup> corresponds to stretching vibration of M-O-M where M corresponds to metal occupying tetrahedral and octahedral. The intense band that in 430 to 550 cm<sup>-1</sup> range in all spectra may be assigned to ZnO stretching.

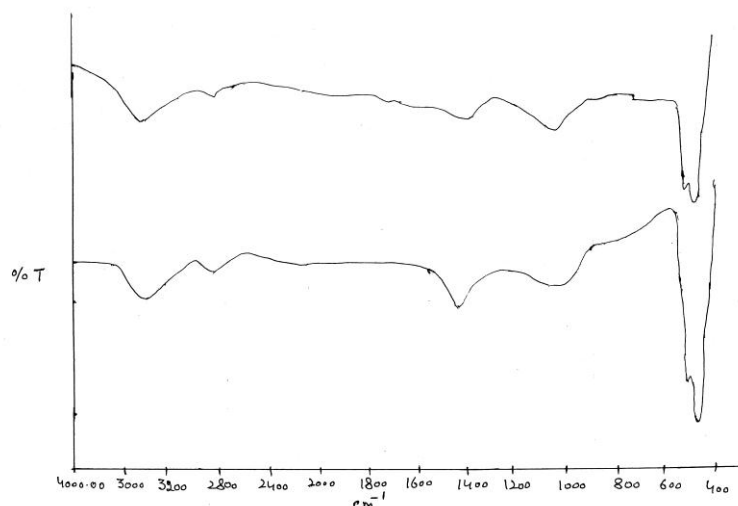


Fig 17: FTIR Spectra of Cu<sub>x</sub>Zn<sub>1-x</sub>O [X= 0.1] calcinated at 600<sup>o</sup>C for 4h and 8h

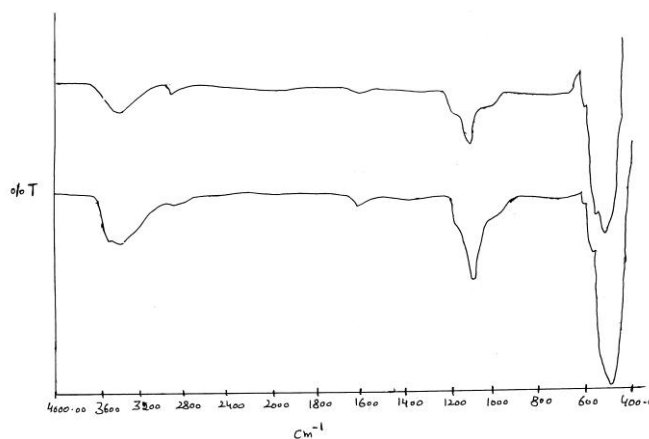


Fig 18: FTIR Spectra of  $\text{Cu}_x\text{Zn}_{1-x}\text{O}$  [X= 0.3] calcinated at  $600^\circ\text{C}$  for 4h and 8h

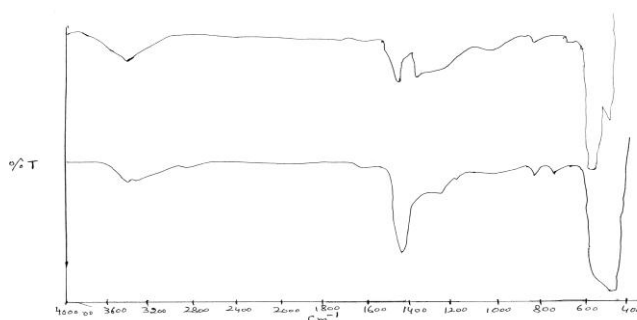


Fig 19: FTIR Spectra of  $\text{Cu}_x\text{Zn}_{1-x}\text{O}$  [X= 0.5] calcinated at  $600^\circ\text{C}$  for 4h and 8h

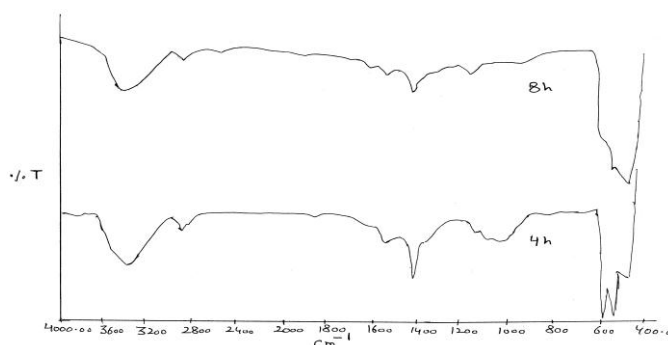


Fig 20: FTIR Spectra of  $\text{Cu}_x\text{Zn}_{1-x}\text{O}$  [X= 0.7] calcinated at  $600^\circ\text{C}$  for 4h and 8h

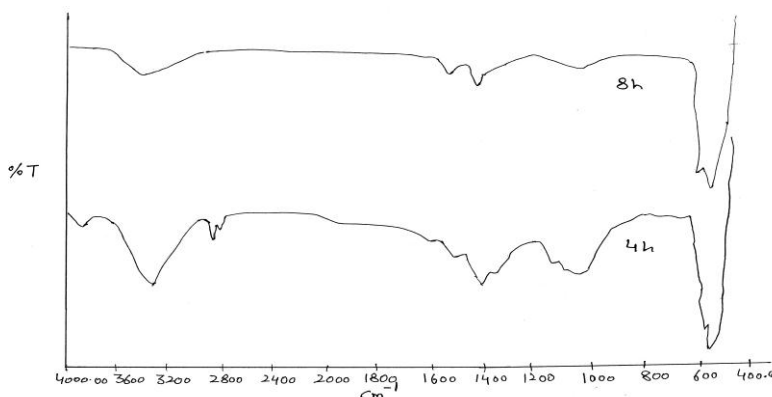


Fig 21: FTIR Spectra of  $\text{Cu}_x\text{Zn}_{1-x}\text{O}$  [X= 0.9] calcinated at  $600^\circ\text{C}$  for 4h and 8h

### CONCLUSION

Nanocomposites  $\text{Cu}_x\text{Zn}_{1-x}\text{O}$  with varying X have been Synthesized successfully using Sol-Gel method..This method is found to be simple and economical. Nano aspect of the nanocomposites is obtained from XRD, SEM. The size of all nanocomposites increases with increasing calcinated time from 4h to 8 h except one with x=0.5 at calcinated temp.  $600^\circ\text{C}$ . In

UV-VIS spectra, it is seen that in all the samples, absorption increases first in ultra violet region and then in visible region with different slopes. It is seen that the value of band gap decreases when we increase the time of calcinations from 4h to 8h in all the samples.

### ACKNOWLEDGEMENT

Author is grateful to UGC for providing the financial support for carrying out research work. Author is grateful to SAIF Punjab University, Chandigarh for characterization like XRD, UV-VIS, FTIR of samples. The author is thankful to Chemistry Dept, M.D. University, Rohtak for providing facility for SEM characterization. The author is thankful to Physics Dept, M.D. University, Rohtak for providing Lab Facilities.

### REFERENCES

- [1] Lieber CM. Solid State Commun 1998; 107:607-616.
- [2] Brune H, Giovannine M, Bromann K. Nature 1998; 394:451-453.
- [3] Chopra L, Major S, Panday DK, Rastogi RS, Vankar VD. Thermal device applications Thin Solid Films 1983; 1021: 1-4.
- [4] Kim H, Gilmore CM. Transparent conducting aluminium doped zinc oxide thin films for organic light emitting device. Appl Phys Letters 2000; 76: 259.
- [5] SK Maji, N Mukherjee, A Mondal, B Adhikary, B Karmakar. Chemical synthesis of mesoporous CuO from a single precursor: Structural, optical and electrical properties. Journal of Solid State Chemistry 2010; 183:1900.
- [6] F Parmigiani and G Samoggia. Experimental Evidence of a Fluctuating Charge State in Cupric Oxide. Europhys Lett 1988; 7: 543.
- [7] XG Zheng, CN Xu, Y Tomokiyo, E Tanaka, H Yamada and Y Soejima. Observation of Charge Stripes in Cupric Oxide. Phys Rev Lett 2000; 85: 5170.
- [8] G Cao, Nanostructures & Nanomaterials: synthesis, Properties & Applications, Imperial College Press, London WC2H 9HE, 2004.
- [9] JL Cao, GS Shao, Y Wang, Y Liu and ZY Yuan. CuO catalysts supported on attapulgite clay for low-temperature CO oxidation. Catal Commun 2008; 9: 2555.
- [10] HP Klung, LE Alexander. X-ray Diffraction Procedures for Polycrystalline and Amorphous Materials, 2nd Edition, Wiley, New York, 1974.
- [11] Hammond C. The Basic of Crystallography and Diffraction ; Oxford University Press; New York, NY, 1997.
- [12] BD Cullity. Element of X-Ray Diffraction, 2ND edn [Addison-Wesley Publishing Company. 1956; 99.
- [13] Zang H et al Biomaterials 2000; 21; 23.
- [14] JI Pancove. Optical Processes in Semiconductors Englewood Cliffs. NJ Prentice Hall 1971.
- [15] RM Silverstein, GC Bassler and TC Morrill. Spectroscopic identification of organic Compounds, John Wiley and Sons, New York, NY 4th Ed, 1984.
- [16] L She, J Zhou, S Gunasekaran: Meter, Letters 2008; 62: 4383.
- [17] Zhang J, Ju X, Wu Z Y et al. Chem Mater 2001; 13: 4192.